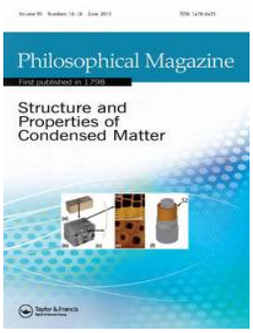

Philosophical Magazine

ISSN: 1478-6435 (Print) 1478-6443 (Online) Journal homepage: http://www.tandfonline.com/loi/tphm20

Characterizing moisture-dependent mechanical properties of organic materials: humidity-controlled static and dynamic nanoindentation of wood cell walls

Luca Bertinetti, Ude D. Hangen, Michaela Eder, Petra Leibner, Peter Fratzl & Igor Zlotnikov

To cite this article: Luca Bertinetti, Ude D. Hangen, Michaela Eder, Petra Leibner, Peter Fratzl & Igor Zlotnikov (2015) Characterizing moisture-dependent mechanical properties of organic materials: humidity-controlled static and dynamic nanoindentation of wood cell walls, Philosophical Magazine, 95:16-18, 1992-1998, DOI: 10.1080/14786435.2014.920544

To link to this article: http://dx.doi.org/10.1080/14786435.2014.920544

Published online: 23 May 2014.

Philosophical Magazine, 2015
Vol. 95, Nos. 16–18, 1992–1998, http://dx.doi.org/10.1080/14786435.2014.920544

Characterizing moisture-dependent mechanical properties of organic materials: humidity-controlled static and dynamic nanoindentation of wood cell walls

Luca Bertinetti[a], Ude D. Hangen[b], Michaela Eder[a], Petra Leibner[a], Peter Fratzl[a] and Igor Zlotnikov[a]*

[a]*Department of Biomaterials, Max Planck Institute of Colloids and Interfaces, Potsdam, Germany;* [b]*Hysitron, Inc., Aachen, Germany*

(*Received 6 January 2014; accepted 28 April 2014*)

Nanoindentation is an ideal technique to study local mechanical properties of a wide range of materials on the sub-micron scale. It has been widely used to investigate biological materials in the dry state; however, their properties are strongly affected by their moisture content, which until now has not been consistently controlled. In the present study, we developed an experimental set-up for measuring local mechanical properties of materials by nanoindentation in a controlled environment of relative humidity (RH) and temperature. The significance of this new approach in studying biological materials was demonstrated for the secondary cell wall layer (S2) in Spruce wood (*Picea abies*). The hardness of the cell wall layer decreased from an average of approximately 0.6 GPa at 6% RH down to approximately 0.2 GPa at 79% RH, corresponding to a reduction by a factor of 3. Under the same conditions, the indentation modulus also decreased by about 40%. The newly designed experimental set-up has a strong potential for a variety of applications involving the temperature- and humidity-dependent properties of biological and artificial organic nanocomposites.

Keywords: biomaterials; wood; relative humidity; nanoindentation; mechanical properties

Introduction

Biological materials are hierarchically structured and typically rather complex nanocomposites [1]. Hence, the understanding of the structure-to-function relationship in these materials at the macroscopic level (bulk) requires studies of all the hierarchical levels at many different length scales, including mechanical characterization on the sub-micron scale. Nanoindentation is an ideal method to characterize mechanical properties of materials at that scale. Since the late 1990s, its application range has been extended to study biological materials such as bone, marine shells, silica sponges, and wood [2–5]. Typically, the experiments are performed in the environmental conditions of the measurement chamber that do not represent the natural state of the biological specimens. Furthermore, the preparation of specimens, which require relatively flat surfaces, often

*Corresponding author. Email: igor.zlotnikov@mpikg.mpg.de

necessitates stabilization by embedding the sample in resin. Normally, the embedding step results in further dehydration, which may cause chemical modification and imposes physical constrain for moisture absorption. The ability to perform nanoindentation under a controlled environment is of particular importance, as biological materials typically reside in humid environments in their natural condition and perform under a variety of relative humidities and temperatures (exoskeletons of arthropods, bone in the human body and wood of a living tree). This is equally important for understanding biological systems in their natural state and their possible applications. So far, an experimental set-up allowing routine nanoindentation experiments to be performed at various levels of relative humidity (RH) and temperatures was not yet technically achieved. For those reasons, the measurements on hygroscopic materials have been attempted only on samples immersed in water (representing 100% of RH) [6–9] or under controlled RH achieved by saturated salt solutions of up to 70% (higher relative humidities cause hardware damage, are very time consuming and condensation inside indentation chamber might prevent moisture equilibration) [10–13].

Here, we present a new experimental set-up which allows humidity- and temperature-controlled static and dynamic nanoindentation experiments. Its importance for biological materials research is demonstrated on the secondary wood cell wall in Spruce wood (*Picea abies*) whose structure and mechanical properties have been studied extensively (including studies by nanoindentation) [2,14–24]. As shown in Figure 1, wood is a complex cellular material (Figure 1(a) and (b)) mainly consisting of long, hollow cells (Figure 1(c)) with different wall thicknesses (Figure 1(d)), which forms alternating layers (growth rings) within a growth season. The cells are held together by the lignin-rich middle lamellae (thin dark areas in Figure 1(e)) and each cell consists of a primary and several secondary layers, Figure 1(f). The secondary cell wall material is comprised of stiff, parallel-aligned cellulose fibrils (indicated by black lines in Figure 1(f)), embedded in a softer matrix of hemicelluloses and lignin. It is well known that cell wall elastic properties are strongly dependent on their moisture content and on the microfibril

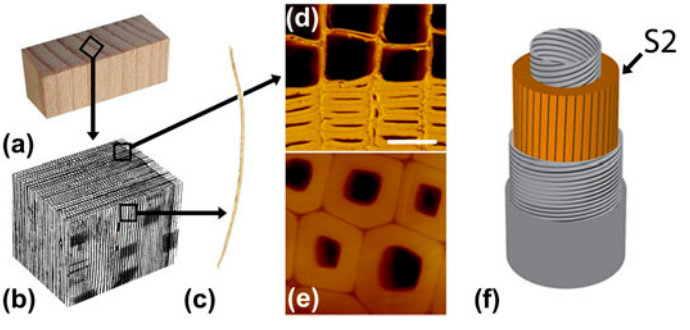

Figure 1. *P. abies* microstructure: (a) optical image of the bulk wood sample; (b) microstructure of wood; (c) single hollow wood cell; (d) environmental scanning electron micrograph of the interface between late (bottom) and early wood (top) regions (scale bar is 40 μm); (e) topographical image of late wood cells obtained by the imaging mode of the nanoindenter, image size is $50 \times 50\ \mu m^2$; (f) schematic representation of a single cell and its comprising layers.

angle (MFA), which is the angle of the cellulose fibrils with respect to the longitudinal cell axis of the predominant S2 layer (orange layer in Figure 1(f)) [25].

Since wood is used for many applications – ranging from outdoor uses to furniture or paper production – an abundance of data demonstrating its hydromechanical and creep properties can be found in literature [13,26]. By the first half of the twentieth century, the mechanical behaviour of macroscopic (bulk) wood was described in detail [27], showing, for example, that the elastic modulus of dry spruce wood (less than 5% moisture content) decreases by ~30% when a moisture content of ~30% (fibre saturation point) is reached [28]. Environmentally controlled static and dynamic mechanical characterization was also performed on isolated single cells. However, even the latter do not reflect pure cell wall properties since the results are affected by geometrical effects, e.g. tension buckling of the helically structured hollow cells [29,30], and by the individual properties of each of the constituting layers, Figure 1(f). In contrast, humidity-controlled nanoindentation of a non-embedded wood material will allow to resolve the moisture-dependent mechanical behaviour of each of the cell wall layers independently. Furthermore, the development of such set-up has the potential to find applications in sub-micron mechanical characterization of all moisture-dependent organic and hybrid nanocomposites.

Experimental section

For humidity- and temperature-controlled nanoindentation experiments, a Triboindenter TI-950 nanoindentation system and a xSol-600 high temperature stage, both produced by Hysitron, Inc., were used. The xSol stage is designed to be mounted inside the nanoindenter chamber and is dedicated to perform measurements at elevated temperatures, up to 600 °C. To avoid oxidation during heating, the stage includes the infrastructure required to create a local inert gas atmosphere. This infrastructure was adapted by us to create an environment with a locally controlled humidity and temperature (Figure 2).

A WETSYS humidity generator (Setaram), which is able to deliver airflow between 50 and 200 ml/min of controlled RH with an accuracy of 0.1%, was connected to the inert gas inlet connected to the lower block of the heating stage. The humid airflow was generated at 32 °C and was routed to the stage inlet via a heated transfer line. The upper block of the heating stage was placed on top of two o-rings isolating the internal space between the blocks from the rest of the indentation chamber and was kept at 24.5 °C. The wood sample was mounted on the lower block directly underneath the slit

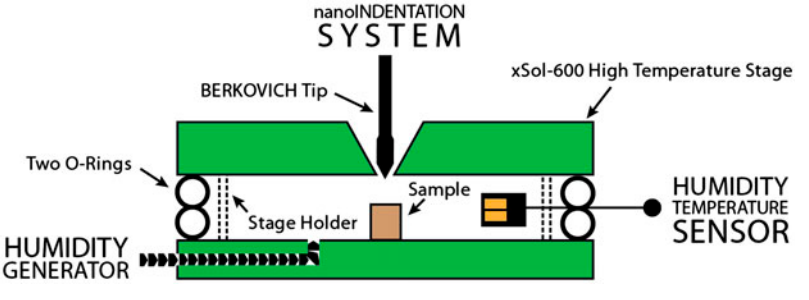

Figure 2. (colour online) A schematic representation of the experimental set-up.

designated for nanoindenter tip insertion. Finally, the actual humidity and temperature inside the measurement chamber were measured with an EK-H4 Evaluation Kit (Sensirion) used with a SHT75 capacitive sensor placed between the two o-rings, a few millimetres away from the sample. The accuracy of the RH and temperature readings was 2% and 0.5 °C, respectively. The humidity stabilization time before each nanoindentation experiment at every RH was approximately 5 h during which the indented volume is expected to be fully equilibrated with the induced environmental conditions.

The indentation experiments were performed on cross-sections of thick (3–7 μm) latewood secondary cell walls (Figure 1) to minimize edge effects [31], since the sample was not embedded. The flat surface was created with a Leica cryo-ultramicrotome on a small area of an ice embedded 5 mm × 5 mm × 5 mm adult Spruce wood block (MFA of S2 layer ~10°) which was then allowed to thaw. The use of cryo-ultramicrotome allowed us to prepare samples with flat surfaces suitable for nanoindentation experiments avoiding embedding it in resin.

All nanoindentation measurements were performed using a long-Berkovich diamond tip with a loading function consisting of a five second loading segment up to a maximal load of 700 μN, followed by a ten second holding segment and finally, a five second unloading segment. The results from 20 indents on at least three different wood cells at every RH were averaged.

Results and discussion

Hardness and reduced modulus measured at four different RHs of 6, 31, 50 and 79% at a constant temperature of 24.5 °C were calculated using the Oliver–Pharr method [32] and plotted in Figure 3(a) (circles). The graph clearly illustrates the effect of RH on the static mechanical properties of the secondary wood cell wall. The reduced modulus obtained at relatively low RHs of 6 and 31% is almost identical – approximately 21 GPa. Increasing the RH resulted in a significant decrease of the reduced modulus to approximately 18 and 13 GPa at RHs of 50 and 79%, respectively. At the same time, hardness of the secondary cell wall exhibited a systematic decrease from an average of approximately 0.6 GPa at 6% RH down to approximately 0.2 GPa at 79% RH, thus, a total decrease of 67% was observed. These data are compared to nanoindentation results measured on a water-submerged *P. abies* specimen representing 100% RH (measured by us, diamonds), to nanoindentation data measured at 60% RH (rectangles) [33] and to a collection of reduced moduli taken from literature measured in a "dry" state (adapted from Ref. [18], pink circle), Figure 3(a). It is important to note that the "dry" state of the measured samples refers to measurements performed in unspecified environmental settings, presumably in a RH range of 30–60%. The large spread in elastic modulus data with respect to hardness is mainly due to the strong dependency of modulus on MFA that varies from cell to cell. The hardness, on the other hand, is dominated by the properties of the matrix [16]. It can be observed that these values fit well to the trend experimentally obtained by humidity-controlled nanoindentation.

The change in plastic behaviour of the secondary wood cell wall as a function of increasing RH, as expressed by the decreasing hardness in Figure 3(a), can be observed in representative load-displacement curves plotted in Figure 3(b). At the same maximal load of 700 μN, the penetration depth and the area under the curves increase significantly with increasing RH. This is accompanied by a twofold increase in the

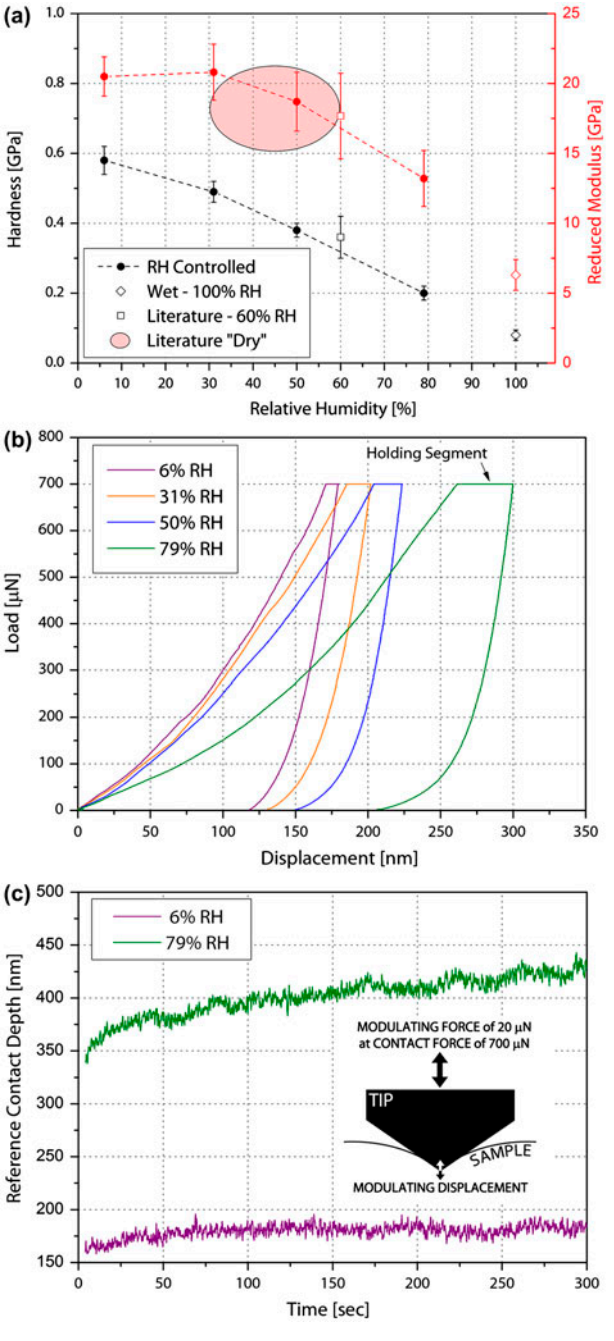

Figure 3. Mechanical properties of the secondary wood cell wall, S2, in *P. abies*: (a) the average hardness and reduced modulus measured in a static nanoindentation mode: at four RHs of 6, 31, 50 and 79% – circles, water submerged specimen representing 100% RH – diamonds, at 60% RH – rectangles (adapted from Ref. [33]) and reduced moduli collected from literature measured in a "dry" state – pink circle (adapted from Ref. [18]); (b) representative load-displacement curves measured in four corresponding RHs of 6, 31, 50 and 79%; (c) representative reference contact depth-time curves measured in a dynamic nanoindentation mode at two RHs of 6 and 79%; the insert is a schematic description of the dynamic nanoindentation measurement mode. © Hysitron Inc.

plastic work done during the nanoindentation experiment and calculated by integrating the area under the curves: approximately 40 and 80 pJ at 6% RH and 79% RH, respectively. In addition, a change in creep behaviour is clearly evident during the 10 s holding segment of the measurement. Despite the higher displacement of the tip at higher RH and therefore, smaller stresses at the contact point, the length of the holding segment increases. For example, comparing the load-displacement curves at 6% RH with 79% RH, an additional creep displacement of approximately 10 and 40 nm, respectively, occurs, suggesting that RH strongly affects the viscous properties of the secondary wood cell wall.

To further investigate the creep behaviour of the S2 layer, dynamic tests were performed. The tip was displaced into the cell wall with a static load of 700 μN and a superimposed modulating load of 20 μN at a frequency of 220 Hz for a total time of 300 s, Figure 3(c). During that time, the change in contact depth was recorded. The resulted representative contact depth-time curves at 6% RH and 79% RH are plotted in Figure 3(c). It can be seen that at 6% RH the contact depth increased by approximately 25 nm and reached an equilibrium state after approximately 50 s. At the same time, at 79% RH, the contact depth increased by almost 100 nm and equilibrium was not reached even after 300 s, clearly demonstrating an increase in viscous behaviour of the secondary wood cell wall with increasing RH. Similar dependency of creep as a function of RH was observed on macroscopic wood samples [13]. Nevertheless, the total amounts of creep and equilibration times are different as these measurements do not represent the behaviour of the secondary cell wall layer alone but of the entire wood.

Conclusions

In conclusion, we successfully designed and realized experimental set-up for environmentally controlled static and dynamic mechanical testing by nanoindentation. This set-up allowed moisture-dependent mechanical properties of the S2 layer of non-embedded *P. abies* cell walls to be exclusively and independently determined. The obtained results show a systematic change in local static and dynamic nanomechanical properties with varying RH corroborating the need for environmentally controlled mechanical characterization methods. This set-up is promising for better comprehension of naturally occurring nanocomposite systems and artificial organic materials and their dependent mechanical response to time, temperature and humidity.

Notes

The authors declare no competing financial interest.

Author contributions

The manuscript was written through contributions of all authors. All authors approved the final version of the manuscript.

References

[1] P. Fratzl and R. Weinkamer, Prog. Mater. Sci. 52 (2007) p.1263.
[2] R. Wimmer, B.N. Lucas, W.C. Oliver and T.Y. Tsui, Wood Sci. Technol. 31 (1997) p.131.

[3] H.S. Gupta, S. Schratter, W. Tesch, P. Roschger, A. Berzlanovich, T. Schoeberl, K. Klaushofer and P. Fratzl, J. Struct. Biol. 149 (2005) p.138.
[4] I. Zlotnikov, D. Shilo, Y. Dauphin, H. Blumtritt, P. Werner, E. Zolotoyabko and P. Fratzl, RSC Adv. 3 (2013) p.5798.
[5] A. Schneider, B. Heiland, N. Peter, C. Guth, E. Arzt and I. Weiss, BMC Biophys. 5 (2012) p.1.
[6] J.Y. Rho and G.M. Pharr, J. Mater. Sci. Mater. Med. 10 (1999) p.485.
[7] C.E. Hoffler, X.E. Guo, P.K. Zysset and S.A. Goldstein, J. Biomech. Eng. 127 (2005) p.1046.
[8] G. Guidoni, J. Denkmayr, T. Schöberl and I. Jäger, Philos. Mag. 86 (2006) p.5705.
[9] G. Guidoni, M. Swain and I. Jäger, Philos. Mag. 90 (2010) p.553.
[10] Y. Yu, B. Fei, H. Wang and G. Tian, Holzforschung 65 (2011) p.121.
[11] L. Farran, A.R. Ennos and S.J. Eichhorn, J. Mater. Res. 24 (2009) p.980.
[12] L. Greenspan, J. Res. NBS Sect. A Phys. Chem. 81 (1977) p.89.
[13] T. Engelund Emil, L. Salmén, Holzforschung 66 (2012) p.959.
[14] W. Gindl and H.S. Gupta, Composites Part A 33 (2002) p.1141.
[15] W. Gindl, H.S. Gupta and C. Grünwald, Can. J. Bot. 80 (2002) p.1029.
[16] W. Gindl, H.S. Gupta, T. Schöberl, H.C. Lichtenegger and P. Fratzl, Appl. Phys. A 79 (2004) p.2069.
[17] W. Gindl and T. Schöberl, Composites Part A 35 (2004) p.1345.
[18] M. Eder, O. Arnould, J.C. Dunlop, J. Hornatowska and L. Salmén, Wood Sci. Technol. 47 (2013) p.163.
[19] Y. Wu, S. Wang, D. Zhou, C. Xing and Y. Zhang, Wood Fiber Sci. 41 (2009) p.64.
[20] W.T.Y. Tze, S. Wang, T.G. Rials, G.M. Pharr and S.S. Kelley, Composites Part A 38 (2007) p.945.
[21] J. Konnerth, N. Gierlinger, J. Keckes and W. Gindl, J. Mater. Sci. 44 (2009) p.4399.
[22] A. Jäger, T. Bader, K. Hofstetter and J. Eberhardsteiner, Composites Part A 42 (2011) p.677.
[23] A. Jäger, K. Hofstetter, C. Buksnowitz, W. Gindl-Altmutter and J. Konnerth, Composites Part A 42 (2011) p.2101.
[24] K. de Borst, T.K. Bader and C. Wikete, J. Struct. Biol. 177 (2012) p.532.
[25] D. Fengel and G. Wegener, *Wood: Chemistry, Ultrastructure, Reactions*, Walter de Gruyter, Berlin, 1984.
[26] E. Engelund, L. Thygesen, S. Svensson and C.S. Hill, Wood Sci. Technol. 47 (2013) p.141.
[27] F. Kollmann, *Technologie des Holzes und der Holzwerkstoffe* [Technology of wood and woodworking material], Vol. 1, Springer-Verlag, Berlin, 1951.
[28] P. Niemz, *Physik des Holzes und der Holzwerkstoffe* [Physics of wood and woodworking material], DRW-Verlag, Stuttgart, 1993.
[29] M. Eder, S. Stanzl-Tschegg and I. Burgert, Wood Sci. Technol. 42 (2008) p.679.
[30] N.J. Pagano, J.C. Halpin and J.M. Whitney, J. Compos. Mater. 2 (1968) p.154.
[31] J.E. Jakes, C.R. Frihart, J.F. Beecher, R.J. Moon, P.J. Resto, Z.H. Melgarejo, O.M. Suárez, H. Baumgart, A.A. Elmustafa and D.S. Stone, J. Mater. Res. 24 (2009) p.1016.
[32] W.C. Oliver and G.M. Pharr, J. Mater. Res. 7 (1992) p.1564.
[33] L. Wagner, T. Bader and K. Borst, J. Mater. Sci. 49 (2014) p.94.